Moveout approximations for P waves in media of monoclinic and higher anisotropy symmetries

Véronique Farra [1] and Ivan Pšenčík [2]

[1]Institut de Physique du Globe de Paris, Sorbonne Paris Cité, Université Paris Diderot, UMR 7154 CNRS, F-75005 Paris, France. E-mail: farra@ipgp.fr
[2]Institute of Geophysics, Acad. Sci. of Czech Republic, Boční II, 141 31 Praha 4, Czech Republic. E-mail: ip@ig.cas.cz

Abstract

We derive and test approximate P-wave moveout formulae for monoclinic, orthorhombic or transversely isotropic media with a vertical or horizontal axis of symmetry underlaid by a horizontal reflector coinciding with a symmetry plane. For the derivation of the formulae, we use the weak-anisotropy approximation, in which deviations of anisotropy from isotropy are assumed to be small. Derived traveltime formulae represent an expansion of traveltime with respect to small parameters characterizing the mentioned deviations. In addition to the traveltime formulae, we also present approximate formulae for normal moveout velocities. All resulting formulae are relatively simple, transparent and described by a reduced number of weak-anisotropy parameters specifying the medium. In monoclinic, orthorhombic or transversely isotropic media, the traveltime formulae depend on 8, 5 or 2 weak-anisotropy parameters. The accuracy of the formulae depends strongly on deviations of ray- and phase-velocity directions. Nevertheless, relative traveltime errors of the most accurate moveout formula do not exceed 1% for anisotropies whose strength is around 25%.

Introduction

As Grechka et al. (2000) point out, there is an abundant geological evidence of the existence of multiple vertical fracture sets (Schoenberg and Sayers, 1995). Media composed of such fracture sets behave as monoclinic, whose plane of symmetry is horizontal. We present the P-wave moveout formulae for such a type of media. For the derivation of the formulae, we use the approach used in our previous papers (Farra and Pšenčík, 2013a,b), in which we dealt with moveout formulae for unconverted reflected P and S waves whose rays were situated in planes of symmetry of TI media. In the former paper, we dealt with transversely isotropic media with the vertical axis of symmetry (VTI), in latter with the so-called dip-constrained transversely isotropic (DTI) media.

In standard approaches, the moveout formulae are derived as an expansion of the

Seismic Waves in Complex 3–D Structures, **24** (2014), 35–58 (ISSN 2336–3827, online at http://sw3d.cz)

square of reflection traveltime T into a Taylor series in terms of the square of the source-receiver offset x (e.g., Thomsen, 1986; Tsvankin and Thomsen, 1994; Stovas, 2010). We propose an alternative way of the derivation of moveout formulae, based on the weak-anisotropy (WA) approximation. We expand T^2 in terms of the weak-anisotropy (WA) parameters, which characterize the deviation of anisotropy from isotropy, and which represent a generalization of Thomsen (1986) parameters to anisotropic media of arbitrary symmetry. In this paper, results obtained by Farra and Pšenčík (2013a,b) are generalized for unconverted reflected P waves propagating in anisotropic media of lower symmetry. We concentrate on situations, in which down-going and up-going parts of rays of the reflected wave are situated in a plane perpendicular to the reflector, and are symmetrical with respect to the normal to this reflector. Such situations occur everywhere, where the properties of the medium repeat after the rotation by π around the normal to the reflector. This corresponds to the situation, in which the reflector represents a symmetry plane of the considered anisotropic medium. Such media include transversely isotropic media with vertical (VTI) or horizontal (HTI) axis of symmetry, orthorhombic media with one of the symmetry planes coinciding with the reflector, and even monoclinic media, whose plane of symmetry coincides with the reflector.

All the derivations in this paper are based on the weak-anisotropy approximation (Farra and Pšenčík, 2003). Instead of using 21 elastic parameters in the Voigt notation we use 21 weak-anisotropy (WA) parameters specified in a global Cartesian coordinate system. Assumption of the weak anisotropy allows us to deal with P waves separately from S waves. Thus the number of WA parameters involved in our formulae is substantially reduced. We derive the expressions for reflection traveltimes and normal moveout (NMO) velocity in two steps. In the first step, we derive them in a local (primed) Cartesian coordinate system related to the source-receiver line. In this coordinate system, the traveltime formulae depend on, at most, 4 local (primed) WA parameters and NMO velocity formula on just one primed parameter. In the second step, we express the primed WA parameters in terms of the WA parameters in the global coordinate system (non-primed). In this way, the reflection traveltime formula depends, in the most general case of a monoclinic medium, on 9 WA parameters (this number can be reduced to 8 if a proper choice of the velocity of the reference isotropic medium is made). The formula for the NMO velocity in a monoclinic medium depends on 3 WA parameters. These numbers reduce if higher symmetry anisotropy or less accurate formulae are used.

The simplest, but also less accurate, are the formulae, in which we neglect the deviation of the ray and slowness vector directions. More accurate formulae are obtained if the deviation of these vectors is taken into account, and even higher accuracy can be obtained if instead of the first-order, second-order approximation of the phase velocity is used. With increasing accuracy, the formulae become slightly more complicated.

We start the paper with the review of basic formulae, which include exact expression for the square of traveltime of an unconverted P-wave reflected from a plane reflector parallel to the plane of symmetry of the overlaying medium as a function of the square of the offset. We describe three possible approaches of evaluation of the traveltime formula. Principal step in all of them is the evaluation of the ray velocity for the direction specified by the slowness vector. In the following section, we use the three approaches and derive corresponding traveltime formulae whose accuracy successively increases. In the final theoretical section, we present normal-moveout velocity formulae corresponding to

the three approaches. Then we study accuracy of the derived formulae on three examples of anisotropic media: HTI, orthorhombic and monoclinic medium. Brief description of obtained results and possible generalizations of the proposed formulae can be found in concluding section. Appendices A and B contain explicit formulae (in global and local coordinates) for a symmetric matrix which plays a basic role in weak-anisotropy approximation. Definition of WA parameters can be also found in Appendix A, transformation relations between WA parameters specified in global and local coordinates can be found in Appendix B.

In the following, the lower-case indices $i, j, k, l, ...$ take the values of 1,2,3, the upper-case indices $I, J, K, L, ...$ take the values of 1,2. The Einstein summation convention over repeated indices is used.

Basic formulae

Let us consider a Cartesian coordinate system whose z-axis is vertical and x- and y-axes are horizontal. Let us further consider a homogeneous layer, which may be transversely isotropic with horizontal or vertical axis of symmetry, orthorhombic or monoclinic. In all cases, let us assume that the horizontal reflector underlying the mentioned layer is parallel to a plane of symmetry. In such a case, down-going and up-going parts of a reflected ray are situated in a vertical plane and in this plane, they are symmetric with respect to the normal to the reflector. As Farra and Pšenčík (2013a), we can thus start the derivations from the exact formula for the square of the traveltime T of an unconverted reflected P wave. The wave propagates from source S to the reflector and then back to receiver R. Points S and R are situated on a horizontal profile parallel to the x'-axis of a local Cartesian coordinate system whose origin coincides with the origin of the global coordinate system x, y, z. Point S is a coordinate origin common for both coordinate systems. The reflected ray is thus situated in vertical plane (x', z'). The square of the exact traveltime along the reflected ray has the form:

$$T^2(x) = \frac{4H^2 + x^2}{v^2(\mathbf{n})} \ . \tag{1}$$

Here x is the offset (distance between S and R) and H is the depth of the horizontal reflector (coinciding with the symmetry plane). $T = T(x)$ denotes the exact traveltime of the considered unconverted reflected P wave. Symbol $v = v(\mathbf{n})$ denotes the ray velocity, which is a function of the direction $\mathbf{n}$ of slowness vector $\mathbf{p} = \mathbf{n}/c$, where c denotes the phase velocity. In the considered configuration, $v(\mathbf{n})$ is the same along the down- and up-going parts of the reflected ray. This simplifies derivations considerably.

We can transform equation (1) using the notation common in moveout analysis:

$$\bar{x} = \frac{x}{2H} \ , \qquad T_0 = \frac{2H}{\alpha_0} \ . \tag{2}$$

Here $\bar{x}$ is the normalized offset, α_0 is the vertical P-wave phase velocity, symbol T_0 denotes the two-way zero-offset traveltime. Using (2), equation (1) can be expressed as:

$$T^2(\bar{x}) = \alpha_0^2 T_0^2 \ \frac{1 + \bar{x}^2}{v^2(\mathbf{n})} \ . \tag{3}$$

In contrast to the situation, in which the reflected ray is situated in a plane of symmetry (Farra and Pšenčík, 2013a,b), vector **n** specifying the direction of slowness vector **p** may deviate from the plane (x', z'), in which the ray is situated. In fact, vector **n** may differ considerably from the corresponding direction **N** of the ray velocity, which specifies the direction of the ray. Vector **N**, which is, in contrast to **n**, situated in the plane (x', z'), can be easily determined from the geometry, which leads to equation (1). Due to the symmetry of the studied problem, it is not important if **N** specifies the direction of the down-going or up-going part of the ray of the reflected P wave. Let us consider the down-going part, for which vector **N**, expressed in terms of the normalized offset $\bar{x}$, has components:

$$N_1' = \frac{\bar{x}}{\sqrt{1+\bar{x}^2}} , \qquad N_2' = 0 , \qquad N_3' = \frac{1}{\sqrt{1+\bar{x}^2}} . \tag{4}$$

For the evaluation of equation (3), we need to find slowness-vector direction **n** corresponding to a given ray-velocity direction **N**. It is relatively simple to determine **N** corresponding to a given **n**. However, to determine **n** corresponding to a given **N** is not such an easy task. To solve it, we can use approximate expressions given by Farra and Pšenčík (2013a).

Farra and Pšenčík (2013a) offer three possible ways of approximate evaluation of (3):

1) Ignore the difference between vectors **n** and **N**. Then, in the first-order approximation, ray velocity v equals phase velocity c:

$$v^2(\mathbf{n}) = c^2(\mathbf{N}) . \tag{5}$$

2) Take the difference between vectors **n** and **N** into account and express the ray velocity in terms of the first-order phase velocity:

$$v^2(\mathbf{n}) = \frac{c^4(\mathbf{N}) - 4[B_{13}^2(\mathbf{N}) + B_{23}^2(\mathbf{N})]}{c^2(\mathbf{N})} . \tag{6}$$

3) Take the difference between vectors **n** and **N** into account and express the ray velocity in terms of the second-order phase velocity:

$$v^2(\mathbf{n}) = \frac{c^4(\mathbf{N}) + 4a[B_{13}^2(\mathbf{N}) + B_{23}^2(\mathbf{N})]}{c^2(\mathbf{N})} . \tag{7}$$

In eq.(7), $a = (r^2 - 3/4)/(1 - r^2)$, $r = \beta_0/\alpha_0$, where α_0 and β_0 can be chosen, e.g., as $\alpha_0^2 = A_{33}$ and $\beta_0^2 = A_{55}$, where $A_{\alpha\beta}$ are density-normalized elastic parameters in the Voigt notation. Symbols B_{ij} in equations (6) and (7) denote elements of matrix **B**, which plays an important role in the approximate expressions describing wave propagation in weakly anisotropic media. Explicit expressions for the elements B_{13}, B_{23} and $B_{33} = c^2$ for a monoclinic medium in the global Cartesian coordinate system x, y, z are given in equations (A4) of Appendix A. In equations (B2) of Appendix B, elements $B_{13}(\mathbf{N})$, $B_{23}(\mathbf{N})$ and $B_{33}(\mathbf{N})$ are expressed in the local coordinate system x', y', z' related to the profile $\overline{SR}$ over the monoclinic medium.

In the following, we use formulae (3) and (4) in the plane (x', z'). It means that in equations (5) - (7), we use B_{13}, B_{23} and $B_{33} = c^2$ from equations (B2) expressed in terms

of primed weak-anisotropy (WA) parameters. Equations (B3) represent transformation relations showing how the primed WA parameters depend on WA parameters (A5) specifying a monoclinic medium. By inserting equations (4) into equations (B2) we obtain expressions for $B_{13}(\mathbf{N})$, $B_{23}(\mathbf{N})$ and $c^2(\mathbf{N}) = B_{33}(\mathbf{N})$ in terms of the normalized offset $\bar{x}$ and primed WA parameters:

$$B_{13}(\bar{x}) = \frac{\alpha_0^2 Q_1(\bar{x})}{2(1+\bar{x}^2)^2} \ , \quad B_{23}(\bar{x}) = \frac{\alpha_0^2 (1+\bar{x}^2)^{1/2} Q_2(\bar{x})}{2(1+\bar{x}^2)^2} \ , \quad c^2(\bar{x}) = \frac{\alpha_0^2 P(\bar{x})}{(1+\bar{x}^2)^2} \ . \tag{8}$$

In equations (8), symbols $P(\bar{x})$, $Q_1(\bar{x})$ and $Q_2(\bar{x})$ denote polynomials:

$$\begin{aligned} P(\bar{x}) &= (1+\bar{x}^2)^2 + 2\delta'_y \bar{x}^2 + 2\epsilon'_x \bar{x}^4 \ , \\ Q_1(\bar{x}) &= 2\bar{x}[2\epsilon'_x \bar{x}^2 + \delta'_y (1-\bar{x}^2)] \ , \\ Q_2(\bar{x}) &= 2\bar{x}(\chi'_z + \epsilon'_{16} \bar{x}^2) \ . \end{aligned} \tag{9}$$

Polynomial $P(\bar{x})$ contains terms of the zero and first order, polynomials $Q_1(\bar{x})$ and $Q_2(\bar{x})$ contain only terms of the first order in the WA parameters. Note that polynomials $P(\bar{x})$ and $Q_1(\bar{x})$ are formally identical with polynomials $P(\bar{x})$ and $Q(\bar{x})$ used by Farra and Pšenčík (2013a; eqs (21), (25)), only ϵ_W and δ_W are replaced here by ϵ'_x and δ'_y.

Traveltime formulae

We have now available all the necessary expressions for all three possible ways of approximate evaluation of the traveltime formula (3) in the plane (x', z').

Case 1

We can express $v^2(\mathbf{n})$ in equation (5) using the third equation of (8), and we get

$$v^2(\mathbf{n}) = \alpha_0^2 \frac{P(\bar{x})}{(1+\bar{x}^2)^2} \ . \tag{10}$$

Inserting equation (10) to (3), we obtain

$$T^2(\bar{x}) = T_0^2 \ \frac{(1+\bar{x}^2)^3}{P(\bar{x})} \ , \tag{11}$$

where $P(\bar{x})$ is given in (9). Using the transformation relations (B3) in the expression for $P(\bar{x})$, equation (11) represents the first-order traveltime formula for a monoclinic medium, in whose derivation we ignored the difference in the orientation of vectors $\mathbf{n}$ and $\mathbf{N}$, and thus considered $v(\mathbf{n}) = c(\mathbf{N})$. Formulae for orthorhombic, HTI or VTI media can be obtained from (11), in which we express the WA parameters ϵ'_x and δ'_y appearing in the polynomial $P(\bar{x})$ using expressions (B5), (B7) or (B9), respectively.

For zero offset, equation (11) yields correctly the square of the two-way zero-offset traveltime T_0. For long offsets, $\lim_{x\to\infty} T^2(x)/x^2$ yields c_H^{-2}, where $c_H^2 = \alpha_0^2(1+2\epsilon'_x)$ is the first-order approximation of the square of the phase velocity in the horizontal direction, see the last equation in (B2).

The approximation (11) depends on four parameters: two-way zero-offset traveltime T_0 related to α_0, the depth H of the reflector and two primed WA parameters ϵ'_x and δ'_y. For $\alpha_0^2 = A_{33}$, these parameters depend, through relations (B3), on 8 WA parameters in monoclinic media, through (B5) on 5 WA parameters in orthorhombic media and through (B7) and (B9) on 2 WA parameters in HTI and VTI media, respectively. For VTI media, the obtained formulae are identical to formulae derived by Farra and Pšenčík (2013a).

Case 2

In this case, we express $v^2(\mathbf{n})$ in equation (6) using equations (8) to get

$$v^2(\mathbf{n}) = \alpha_0^2 \frac{P^2(\bar{x}) - Q_1^2(\bar{x}) - (1+\bar{x}^2)Q_2^2(\bar{x})}{P(\bar{x})(1+\bar{x}^2)^2} \ . \tag{12}$$

Inserting equation (12) to (3), we obtain

$$T^2(\bar{x}) = T_0^2 \ \frac{P(\bar{x})(1+\bar{x}^2)^3}{P^2(\bar{x}) - Q_1^2(\bar{x}) - (1+\bar{x}^2)Q_2^2(\bar{x})} \ . \tag{13}$$

Polynomials $P(\bar{x})$, $Q_1(\bar{x})$ and $Q_2(\bar{x})$ are given in (9). Inserting (B3) to (13), we obtain again the first-order traveltime formula for a monoclinic medium, but in equation (13), we take into account the difference in orientation of vectors $\mathbf{n}$ and $\mathbf{N}$ and express the ray velocity in terms of the first-order phase velocity.

The approximation (13) depends on six parameters: two-way zero-offset traveltime T_0 related to α_0, the depth H of the reflector and four primed WA parameters ϵ'_x, δ'_y, χ'_z and ϵ'_{16}. The number of WA parameters, on which equation (13) depends in media of varying anisotropy symmetry, is the same as in the case of equation (11). For VTI media, we obtain again formulae derived by Farra and Pšenčík (2013a).

Case 3

In this case, we express $v^2(\mathbf{n})$ in equation (7) using equations (8) to get

$$v^2(\mathbf{n}) = \alpha_0^2 \frac{P^2(\bar{x}) + a[Q_1^2(\bar{x}) + (1+\bar{x}^2)Q_2^2(\bar{x})]}{P(\bar{x})(1+\bar{x}^2)^2} \ . \tag{14}$$

Inserting equation (14) to (3), we obtain

$$T^2(\bar{x}) = T_0^2 \ \frac{P(\bar{x})(1+\bar{x}^2)^3}{P^2(\bar{x}) + a[Q_1^2(\bar{x}) + (1+\bar{x}^2)Q_2^2(\bar{x})]} \ . \tag{15}$$

Here again, $a = (r^2 - 3/4)/(1-r^2)$ and $r = \beta_0/\alpha_0$. Polynomials $P(\bar{x})$, $Q_1(\bar{x})$ and $Q_2(\bar{x})$ are given in (9). Inserting (B3) to (15), we obtain the second-order traveltime formula for a monoclinic medium, which takes into account the difference in orientation of vectors $\mathbf{n}$ and $\mathbf{N}$ and the expression for the ray velocity in terms of the second-order phase velocity.

The approximation (15) depends on seven parameters: two-way zero-offset traveltime T_0 related to α_0, the depth H of the reflector, four primed WA parameters ϵ'_x, δ'_y, χ'_z,

ϵ'_{16} and parameter $r = \beta_0/\alpha_0$. As in the VTI case studied by Farra and Pšenčík (2013a), the dependence on r is, however, very weak and thus if r is chosen close to the Poisson ratio, i.e., $r^2 \sim 1/3$ ($a \sim -5/8$), it is not necessary to consider it as a free parameter. The number of WA parameters, on which equation (15) depends in media of various anisotropic symmetries, is the same as in the case of equation (11). For VTI media, we obtain formulae derived in Farra and Pšenčík (2013a).

Normal moveout velocity formulae

The above traveltime formulae can be used for the derivation of NMO velocities v_{NMO} of varying accuracy, depending on the accuracy of the used traveltime formula. NMO velocity can be determined from the formula

$$v_{NMO}^{-2} = \frac{dT^2}{dx^2}\Big|_{x=0} , \tag{16}$$

see, e.g., Thomsen (1986). If we use eq.(11) in eq.(16), we obtain

$$v_{NMO}^{-2} = \alpha_0^{-2}(1 - 2\delta'_y) . \tag{17}$$

Equation (17) gives the first-order approximation of the square of NMO velocity in monoclinic media for the case that the difference between vectors **n** and **N** is ignored. This equation coincides with eq.(41) of Pšenčík and Gajewski (1998) and corresponds, within the first order, to the first-order expression for NMO velocity given in eq.(8) of Rasolofosaon (2000). The coincidence is understandable since both references present first-order expressions for an arbitrary, but weak, anisotropy. Equation (17) for a monoclinic medium thus represents their specific case. From (17), we can see that the NMO velocity is varying with azimuth. For monoclinic media, the variation is described by the dependence of the primed WA parameter δ'_y on the WA parameters δ_x, δ_y and χ_z, see equation (B3). For orthorhombic media, the variation of v_{NMO} with azimuth is described by the dependence of δ'_y on δ_x and δ_y, see equation (B5), and for HTI media by the dependence of δ'_y on δ_y, see (B7). From (B9), we can see that, as expected, v_{NMO} does not depend on the azimuth in VTI media.

If we use eq.(13) in eq.(16), we obtain

$$v_{NMO}^{-2} = \alpha_0^{-2}[1 - 2\delta'_y + 4\Big((\delta'_y)^2 + (\chi'_z)^2\Big)] . \tag{18}$$

This is again the first-order NMO velocity, but in this case, the difference between vectors **n** and **N** is considered, and, thus, the expression is more accurate. Its azimuthal dependence is more complicated than in equation (17) because v_{NMO} depends on an additional primed WA parameter χ'_z.

Finally, if we use eq.(15) in eq.(16), we obtain the second-order expression for the NMO velocity

$$v_{NMO}^{-2} = \alpha_0^{-2}[1 - 2\delta'_y - 4a\Big((\delta'_y)^2 + (\chi'_z)^2\Big)] , \tag{19}$$

where again, $a = (r^2 - 3/4)/(1 - r^2)$. In vertical symmetry planes of orthorhombic media, eq.(19) yields second-order approximation of Tsvankin's (1997) exact NMO-velocity formula (36).

We can see that expressions (18) and (19) differ from expression (17) by additional terms of second order in WA parameters. Expressions (17) and (18) represent the first-order and expression (19) represents the second-order approximation of the exact NMO velocity for monoclinic or higher symmetry media.

Let us note that after expressing primed WA parameters in equations (17) - (19) in terms of WA parameters (A5), using transformation relations of Appendix B, we can rewrite NMO velocity formulae in the form:

$$v_{NMO}^{-2} = W_{11}\cos^2\varphi + 2W_{12}\cos\varphi\sin\varphi + W_{22}\sin^2\varphi \ , \tag{20}$$

see, e.g., eq.(3.53) of Tsvankin (2001). In equation (20), angle φ is the azimuth measured from the x-axis of the global coordinate system towards the y-axis. If we insert δ_y' from (B3) to eq.(17), we can rewrite equation (17) to the form (20), in which:

$$W_{11} = \alpha_0^{-2}(1-2\delta_y) \ , \quad W_{12} = -2\alpha_0^{-2}\chi_z \ , \quad W_{22} = \alpha_0^{-2}(1-2\delta_x) \ . \tag{21}$$

This is identical to equation (43) of Pšenčík and Gajewski (1998) and equal, to the first order, to equations (8) and (B-1) of Rasolofosaon (2000). Equations in the mentioned references are of the first order and hold for arbitrary anisotropic symmetry. If we rewrite equation (19) into the form (20) and use the transformation relation for δ_y' and χ_z' from (B3), the coefficients W_{IJ} read:

$$\begin{aligned} &W_{11} = \alpha_0^{-2}[1-2\delta_y-4a(\delta_y^2+\chi_z^2)] \ , \quad W_{12} = -2\alpha_0^{-2}\chi_z[1+2a(\delta_x+\delta_y)] \ , \\ &W_{22} = \alpha_0^{-2}[1-2\delta_x-4a(\delta_x^2+\chi_z^2)] \ . \end{aligned} \tag{22}$$

Equation (20) with coefficients (22) represents an alternative form of the second-order approximation (19) of the NMO velocity for monoclinic media. Coefficients (22) represent second-order approximations of exact coefficients derived by Grechka et al. (2000). They thus give better approximation than coefficients given in eq.(26) of Grechka et al. (2000), which are of the first order. The NMO velocity in a monoclinic medium depends on three WA parameters δ_x, δ_y, χ_z and angle φ.

In orthorhombic media, coefficients (21) or (22) reduce for the specification (B4), i.e., for the planes of symmetry coinciding with coordinate planes, to:

$$W_{11} = \alpha_0^{-2}(1-2\delta_y) \ , \quad W_{12} = 0 \ , \quad W_{22} = \alpha_0^{-2}(1-2\delta_x) \ . \tag{23}$$

or

$$W_{11} = \alpha_0^{-2}[1-2\delta_y(1+2a\delta_y)] \ , \quad W_{12} = 0 \ , \quad W_{22} = \alpha_0^{-2}[1-2\delta_x(1+2a\delta_x)] \ . \tag{24}$$

The NMO velocity thus depends on only two WA parameters δ_x and δ_y and on angle φ.

The NMO-velocity formula simplifies considerably for HTI media. For the specification (B6), i.e., for the axis of symmetry parallel to the x-axis, eqs (20), (22) and equation for δ_y' in (B7) yield:

$$v_{NMO}^{-2} = \alpha_0^{-2}[1-2\delta_y\cos^2\varphi(1+2a\delta_y)] \ . \tag{25}$$

Of course, equation (25) also results from equation (19) and equation for δ_y' in (B7).

In the VTI medium we obtain the second-order expression:

$$v_{NMO}^{-2} = \alpha_0^{-2}[1 - 2\delta_y(1 + 2a\delta_y)] \ , \tag{26}$$

which has already been derived by Farra and Pšenčík (2013a).

Tests of accuracy

Here we test the accuracy of some of the above proposed formulae. We check the relative travel time errors $(T - T_{ex})/T_{ex} \times 100\%$ of formulae (11), (13) and (15). Here T is the approximate traveltime calculated from the formulae presented in a previous section, T_{ex} is the traveltime calculated using the package ANRAY (Gajewski and Pšenčík, 1990), which we consider to be an exact reference. We test the above formulae on models with varying anisotropy symmetry and strength. As a measure of P-wave anisotropy strength, we use the relation $2(V_{max} - V_{min})/(V_{max} + V_{min}) \times 100\%$. Although the models are derived from models for realistic media, they are designed just for testing.

Three models consisting of a homogeneous horizontal layer underlaid by a horizontal reflector are considered. In all of them, reflectors coincide with planes of symmetry of the overlaying medium. The HTI model with axis of symmetry parallel with the x-coordinate axis is derived from the Greenhorn shale model (Stovas, 2010), by making the vertical axis of symmetry horizontal. Farra and Pšenčík (2013a,b) used this model in their study of moveout in TI media with vertical axis of symmetry and in dip-constrained TI media. P-wave anisotropy of this model is rather strong, about 26%. The ORT model is the model used by Schoenberg and Helbig (1997) in their study. Its planes of symmetry coincide with coordinate planes and one of them is parallel to the reflector. P-wave anisotropy of this model is $\sim 25\%$. The third, monoclinic MONO model, was derived from the Vosges sandstone model of Mensch and Rasolofosaon (1997) by making the originally triclinic model monoclinic. Its single plane of symmetry coincides with the reflector. P-wave anisotropy is $\sim 15\%$. P-wave WA parameters of all three models are given in Table 1. WA parameter ϵ_z is zero in all models. Note that to describe P-wave behaviour in the HTI model, we need 3, in the ORT model 6 and in the MONO model 9 WA parameters (including $\epsilon_z = 0$) while in exact formulae, 4, 9 and 12 elastic parameters are necessary, respectively.

Figure 1 shows the relative P-wave traveltime errors for the HTI model versus the normalized offset $\bar{x} = x/2H$. Similarly as traveltimes themselves, the errors vary with azimuth φ. Since the variations with azimuth are quite pronounced, we show traveltime error curves for a dense system of azimuths. Curves of different colours correspond to different azimuths. In the left column, traveltime errors for azimuths $\varphi = 0^o$, 30^o, 45^o, 50^o, and in the right column for $\varphi = 60^o$, 70^o, 80^o and 90^o are shown. The azimuths are measured from the x-axis, which is parallel to the symmetry axis. The plots at the top correspond to the first-order equation (11) ignoring different directions of $\mathbf{N}$ and $\mathbf{n}$. In the middle, the first-order equation (13) taking into account different directions of $\mathbf{N}$ and $\mathbf{n}$ and at the bottom, the second-order equation (15) is used. As expected, we can observe increasing accuracy of results from the top to the bottom. While maximum errors of equation (11) are around 2.5%, for equation (13), they are less than 2% and for equation (15) they are around 0.7%.

Best results with all formulae are obtained, of course, in the isotropy plane, perpen-

dicular to the axis of symmetry, i.e., for $\varphi = 90^o$. This is obvious because squares of all ray-velocity approximations yield α_0^2 in this case. Except for the interval of $\bar{x} \sim 0 - 2$, very good results are also obtained along the profile $\varphi = 0^o$. With increasing deviations of profiles from $\varphi = 0^o$, larger errors extend to larger offsets. For $\varphi \sim 45 - 60^o$, the errors are maximum, for larger azimuths, they successively decrease to zero for $\varphi = 90^o$. As in the VTI case (Farra and Pšenčík, 2013a), this behaviour is closely related to deviations of phase- and ray-velocity vectors, i.e., to deviations of vectors $\mathbf{n}$ and $\mathbf{N}$. They are shown in Figure 2.

In Figure 2, at the top, we can see behaviour of exact phase and ray velocities as functions of the normalized offset $\bar{x}$ along selected profiles. For each profile specified by a colour, we can detect two curves. The upper curve corresponds to the ray velocity, the lower one to the phase velocity. For all azimuths, except $\varphi = 90^o$, which corresponds to the plane of isotropy, we can observe rather strong decrease of both velocities at small offsets. At offsets greater than $\bar{x} \sim 2$, velocities are nearly constant. The strength of the variation at small offsets decreases with increasing azimuth φ. In the middle row of Figure 2, we can observe variation of deviations of exact vectors $\mathbf{N}$ and $\mathbf{n}$ with the normalized offset. We can see that, as in the VTI case studied by Farra and Pšenčík (2013a), the maximum deviations can reach 16^o. For the azimuth $\varphi = 0^o$, the interval of great deviations is rather narrow; for offsets $\bar{x} > 3$ the deviations of $\mathbf{N}$ and $\mathbf{n}$ are negligible. With increasing azimuth, the offsets with large deviations extend, most for $\varphi = 60 - 70^o$. For larger azimuths, the size of the deviations decreases, but it remains high for all offsets. For $\varphi = 90^o$, the deviation is, of course, zero.

The bottom plot in Figure 2 shows variation of NMO velocity with azimuth, for $\varphi = 0^o - 180^o$. Results of the first-order formula (17) with (B7), in which different directions of $\mathbf{N}$ and $\mathbf{n}$ are ignored, are shown in blue, results of second-order formula (19) with (B7) are in red. Exact variation of the NMO velocity with azimuth (black) is shown for comparison. All three NMO velocity curves coincide for azimuth of 90^o (isotropy plane), maximum differences being along the axis of symmetry. The accuracy of the above proposed formulae depends on several factors. First, it is the strength of the anisotropy because the formulae are derived under the assumption of weak anisotropy. Anisotropy of the HTI model is $\sim 26\%$, which cannot be considered weak. From equation (25), we can see that the approximate values of NMO velocity vary around the value of α_0 of the P-wave vertical velocity. The magnitude of the variations is controlled by parameter δ_y, which is, in this case, quite large, see Table 1. In fact, δ_y is considerably larger in the HTI model than in the remaining models. Since the maximum NMO velocity (3.804 km/s) associated with azimuth $\varphi = 90^o$ coincides with the vertical P-wave velocity α_0, the deviations of approximate values of v_{NMO} for azimuths close to 0^o and 180^o are emphasized. The exact NMO velocity is 2.46 km/s in this case while eq.(17) yields 2.88 km/s (blue) and eq.(19) 2.6 km/s (red).

Figure 3 shows results for the ORT model. In the left column, we can see the relative P-wave traveltime errors versus the normalized offset $\bar{x}$ obtained from formulae (11) at the top, (13) in the middle and (15) at the bottom. We can see that in contrast to HTI model, the variation of errors with offset is very similar for all considered azimuths. The decrease of maximum errors with the use of more accurate formulae is similar to that in the HTI case. Maximum errors obtained with equation (11) are approximately 2.8%, they are around 2% for equation (13) and do not exceed 0.6% for equation (15).

In the top plot of the right column of Figure 3, we can see exact phase and ray velocities as functions of the normalized offset $\bar{x}$ along selected profiles. As in Figure 2, for each profile specified by a colour, we can detect two curves. The upper curve corresponds to the ray velocity, the lower one to the phase velocity. In contrast to the HTI case, velocities increase with offset, the increase being more moderate than the decrease in the HTI case. Close to $\bar{x} = 0$, velocities in some azimuths slightly decrease before they start to rise. Variation of curves with azimuth is not so pronounced as in the HTI case, specifically in the top plot of the right column of Figure 2. The first impression from the plot of deviations of vectors $\mathbf{n}$ and $\mathbf{N}$ (middle plot of the right column) is that their variation with the normalized offset changes little with the azimuth. Maximum deviation for azimuths $\varphi = 0^o$ and 90^o is even slightly larger than in the HTI case, approximately 17^o. For azimuth $\varphi = 90^o$ (red), we can observe a change of mutual positions of vectors $\mathbf{n}$ and $\mathbf{N}$ at about $\bar{x} = 0.3$ (the angle between $\mathbf{n}$ and $\mathbf{N}$ changes from negative to positive).

The bottom plot of the right column in Figure 3 shows variation of NMO velocity with azimuth, for $\varphi = 0^o - 180^o$. Results of the first-order formula (17) are again in blue, results of second-order formula (19) in red. Exact variation of the NMO velocity with azimuth is in black. Although anisotropy of the ORT model is also rather strong, about 25%, the formulae (17) and (19) approximate the variation of the exact NMO velocity better than in the HTI case. In case of the formula (19), we can even observe coincidence of the approximate and exact curves. The reasons are a considerably smaller value of δ_y than in the HTI case, see Table 1, and the value of the vertical P-wave velocity, $\alpha_0 = 2.437$ km/s. In contrast to the HTI case, the value of α_0 is situated between NMO velocities for azimuths $\varphi = 0^o$ and 90^o. Exact NMO velocities for these azimuths are 2.239 and 2.629 km/s, respectively. Corresponding values obtained with formula (17) are 2.258 and 2.651 km/s, and 2.242 and 2.628 km/s with formula (19), respectively.

Figures 4 and 5 show results for the MONO model. In Figure 4, we can see that, as in the case of HTI model, the curves of the relative errors versus normalized offset vary quite significantly with azimuth. Maximum errors are considerably smaller than in the HTI case (anisotropy of MONO model is "only" about 15%). In the quadrant from 0^o to 90^o, they are around 1% for the first-order formulae (11) and (13) and slightly more than 0.1% for the second-order formula (15). In the quadrant from 90^o to 180^o, they are higher, about 1.6% for formulae (11) and (13) and about 0.4% for formula (15). Of course, the curves for azimuths 0^o and 180^o are identical. Minimum relative errors can be observed between azimuths 30^o and 45^o, and around 120^o.

Variation of ray and phase velocities with the normalized offset shown at the top of Figure 5 is similar to the variation of velocities in HTI model for azimuths from 0^o to 50^o. The drop of velocities, however, is more moderate. Variation of corresponding deviations of vectors $\mathbf{n}$ and $\mathbf{N}$ with $\bar{x}$ in the middle row of Figure 5 differs from the variation in HTI model. Maximum deviation is only about 14^o (anisotropy of MONO model is about 15%!). Variations also depend less on the azimuth than in the HTI case. As in Figure 4, the curves corresponding to azimuths 0^o and 180^o are identical.

The bottom plot in Figure 5 shows again variation of NMO velocity with azimuth, for $\varphi = 0^o - 180^o$. First-order formula (17) shown in blue, yields highly accurate results around $\varphi = 150^o$. Greatest deviations can be observed for $\varphi = 60^o$. But they are considerably smaller than the deviations in Figure 2. Second-order formula (19), shown

in red, yields results nearly identical with exact (black).

Conclusion

We presented approximate moveout formulae for unconverted reflected P waves for monoclinic, orthorhombic and transversely isotropic media with horizontal or vertical axis of symmetry. In all cases, the horizontal reflector coincided with a symmetry plane of the considered medium. In contrast to currently used Taylor expansions with respect to the offset, we used weak-anisotropy approximation for the derivation of formulae of varying accuracy. In addition to traveltime formulae, we also presented corresponding approximate formulae for NMO velocity. All these formulae depend on the reduced number of parameters specifying the medium. For the vertical P-wave velocity α_0 chosen as $\alpha_0^2 = A_{33}$, which leads to elimination of one of the WA parameters (it becomes identically zero), one needs 8, 5 or 2 WA parameters to describe P-wave behaviour in a monoclinic, orthorhombic or transversely isotropic medium, respectively. In corresponding exact formulae, one needs 12, 9 or 4 elastic parameters.

The proposed formulae were tested on models of varying anisotropy symmetry and anisotropy strength. The tests indicated that accuracy of the formulae does not depend on the anisotropy symmetry. It exhibits certain dependence on the strength of anisotropy. The tests, however, indicated clearly a strong dependence of the accuracy of the formulae on the deviation of phase- and ray-velocity directions. This phenomenon has already been observed in previous studies (Farra and Pšenčík, 2013a, b). Despite of this, the tests showed that especially the second-order traveltime formula yields results with a high accuracy: the maximum relative traveltime errors are well below 1% for anisotropy around 25%.

The presented formulae allow further generalizations. For example, it is possible to generalize the derived formulae to models of dip-constrained media. The generalization can be done in a similar way, in which Farra and Pšenčík (2013b) generalized the results for VTI media to dip-constrained TI media. Another possible generalization is the derivation of similar formulae for S waves. In weakly anisotropic media, S waves usually propagate coupled. For such a case, it would be possible to use the common S-wave ray concept (Bakker, 2002; Klimeš, 2006; Farra and Pšenčík, 2008, 2010) and generalize the P-wave formulae presented in this paper for coupled S waves.

Acknowledgement

A substantial part of this work was done during IP's stay at the IPG Paris at the invitation of the IPGP. We are grateful to project "Seismic waves in complex 3-D structures" (SW3D) and Research Project 210/11/0117 of the Grant Agency of the Czech Republic for support.

Appendix A

Matrix **B** *and WA parameters in global Cartesian coordinates*

Let us consider a global Cartesian coordinate system with the z-axis vertical, positive downwards. The elements B_{ij} of matrix **B** used in the approximate expressions in the text are given by the formula

$$B_{mn}(\mathbf{n}) = a_{ijkl} n_j n_l e_i^{[m]} e_k^{[n]}. \qquad (A1)$$

Here a_{ijkl} are density-normalized elastic moduli (elements of the stiffness tensor). Symbols n_i denote components of a unit vector **n**. Unit, mutually perpendicular vectors $\mathbf{e}^{[i]}$ are defined in the following way:

$$\mathbf{e}_i^{[1]} \equiv D^{-1}(n_1 n_3, n_2 n_3, n_3^2 - 1), \quad \mathbf{e}_i^{[2]} \equiv D^{-1}(-n_2, n_1, 0), \quad \mathbf{e}_i^{[3]} = n_i \equiv (n_1, n_2, n_3), \quad (A2)$$

where

$$D = (n_1^2 + n_2^2)^{1/2}, \quad n_1^2 + n_2^2 + n_3^2 = 1. \qquad (A3)$$

Explicit expressions for elements of matrix **B** for a weakly anisotropic medium of arbitrary symmetry in terms of 21 WA parameters were introduced in Farra and Pšenčík (2003). In case of P waves, it is sufficient to deal with only 3 elements, namely with B_{13}, B_{23} and B_{33}. These elements depend on only 15 (P-wave) WA parameters in the case of most general anisotropy. If we express the elements B_{mn} in terms of the unit vector **n**, then element $B_{33}(\mathbf{n})$ represents square of the phase velocity $c^2(\mathbf{n})$.

In monoclinic media, the number of WA parameters specifying P-wave propagation reduces from 15 to 9. The elements B_{13}, B_{23} and B_{33} attain the following form:

$$B_{13}(\mathbf{n}) = \alpha_0^2 D^{-1}\Big(n_3^3(\eta_y n_1^2 + \eta_x n_2^2 + 2\chi_z n_1 n_2) + n_3[(2\eta_z - \eta_x - \eta_y) n_1^2 n_2^2$$

$$+2(2\epsilon_{16} - \chi_z) n_1^3 n_2 + 2(2\epsilon_{26} - \chi_z) n_1 n_2^3 - \eta_y n_1^4 - \eta_x n_2^4 + (\epsilon_x - \epsilon_z) n_1^2 + (\epsilon_y - \epsilon_z) n_2^2]\Big),$$

$$B_{23}(\mathbf{n}) = \alpha_0^2 D^{-1}\Big(n_3^2[(\eta_x - \eta_y) n_1 n_2 + \chi_z n_1^2 - \chi_z n_2^2]$$

$$+\eta_z n_1^3 n_2 - \eta_z n_1 n_2^3 + 3(\epsilon_{26} - \epsilon_{16}) n_1^2 n_2^2 + \epsilon_{16} n_1^4 - \epsilon_{26} n_2^4 + (\epsilon_y - \epsilon_x) n_1 n_2\Big),$$

$$B_{33}(\mathbf{n}) = c^2(\mathbf{n}) = \alpha_0^2\Big(1 + 2[n_3^2(\eta_y n_1^2 + \eta_x n_2^2 + 2\chi_z n_1 n_2 + \epsilon_z)$$

$$+\epsilon_x n_1^2 + \epsilon_y n_2^2 + \eta_z n_1^2 n_2^2 + 2\epsilon_{16} n_1^3 n_2 + 2\epsilon_{26} n_1 n_2^3]\Big). \qquad (A4)$$

The symbol α_0 in (A4) denotes the P-wave velocity in a reference isotropic medium.

The WA parameters used in (A4) have the following meaning:

$$\epsilon_x = \frac{A_{11} - \alpha_0^2}{2\alpha_0^2}, \quad \epsilon_y = \frac{A_{22} - \alpha_0^2}{2\alpha_0^2}, \quad \epsilon_z = \frac{A_{33} - \alpha_0^2}{2\alpha_0^2},$$

$$\delta_x = \frac{A_{23} + 2A_{44} - \alpha_0^2}{\alpha_0^2}, \quad \delta_y = \frac{A_{13} + 2A_{55} - \alpha_0^2}{\alpha_0^2}, \quad \delta_z = \frac{A_{12} + 2A_{66} - \alpha_0^2}{\alpha_0^2},$$

$$\chi_z = \frac{A_{36} + 2A_{45}}{\alpha_0^2}, \quad \epsilon_{16} = \frac{A_{16}}{\alpha_0^2}, \quad \epsilon_{26} = \frac{A_{26}}{\alpha_0^2}, \qquad (A5)$$

where $A_{\alpha\beta}$ are density normalized elastic parameters in the Voigt notation.

In (A4), the following variables are also used:

$$\eta_x = \delta_x - \epsilon_y - \epsilon_z, \quad \eta_y = \delta_y - \epsilon_x - \epsilon_z, \quad \eta_z = \delta_z - \epsilon_x - \epsilon_y. \qquad (A6)$$

Appendix B

Matrix **B** *and WA parameters along a profile*

Let us consider a local Cartesian coordinate system x', y', z', whose z'-axis coincides with the z axis of the global coordinate system, and both systems have a common origin. The axis x' makes an angle φ with the x-axis in the horizontal plane. Transformation between the two coordinate systems is controlled by the rotation matrix:

$$\begin{pmatrix} \cos\varphi & \sin\varphi & 0 \\ -\sin\varphi & \cos\varphi & 0 \\ 0 & 0 & 1 \end{pmatrix}. \qquad (B1)$$

Let us consider a monoclinic or higher symmetry medium underlaid by a reflector, which coincides with a symmetry plane of the considered medium. In such a model, a ray of a reflected unconverted P wave is confined to a vertical plane and down-going and up-going parts of the ray are symmetrical with respect to the normal to the reflector. Let us consider, for example, the down-going part of such a ray and let us assume that it is situated in the vertical plane (x', z'). The direction of the ray is specified by the unit vector $\mathbf{N} \equiv (N_1', 0, N_3')$. Components of vector $\mathbf{N}$ are expressed in the local Cartesian coordinates x', y', z'. The elements $B_{13}(\mathbf{N})$, $B_{23}(\mathbf{N})$ and $B_{33}(\mathbf{N}) = c^2(\mathbf{N})$ required in equations (5) - (7) can be determined from expressions (A1). If we consider $\alpha_0^2 = A_{33}$, and thus $\epsilon_z = 0$, and $D = |N_1'|$, we get from (A4):

$$B_{13}(\mathbf{N}) = \alpha_0^2 N_1' N_3' [\delta_y' - 2(\delta_y' - \epsilon_x') N_1'^2],$$

$$B_{23}(\mathbf{N}) = \alpha_0^2 N_1' (\chi_z' N_3'^2 + \epsilon_{16}' N_1'^2),$$

$$c^2(\mathbf{N}) = B_{33}(\mathbf{N}) = \alpha_0^2 \Big(1 + 2N_1'^2 [\epsilon_x' + (\delta_y' - \epsilon_x') N_3'^2]\Big). \qquad (B2)$$

Monoclinic media

We can see that expressions (B2) for monoclinic media depend on 4 primed WA parameters ϵ_x', δ_y', χ_z' and ϵ_{16}'. They are related to 8 of 9 WA parameters (remember, $\epsilon_z = 0$) given in (A5). The transformation relations read:

$$\epsilon_x' = \epsilon_x \cos^4\varphi + 2\epsilon_{16} \cos^3\varphi \sin\varphi + \delta_z \cos^2\varphi \sin^2\varphi + \epsilon_y \sin^4\varphi + 2\epsilon_{26} \cos\varphi \sin^3\varphi,$$

$$\delta_y' = \delta_y \cos^2\varphi + 2\chi_z \sin\varphi \cos\varphi + \delta_x \sin^2\varphi,$$

$$\chi'_z = \chi_z \cos 2\varphi + (\delta_x - \delta_y) \sin\varphi \cos\varphi,$$
$$\epsilon'_{16} = -2\epsilon_x \cos^3\varphi \sin\varphi + 2\epsilon_y \sin^3\varphi \cos\varphi + \delta_z \cos\varphi \sin\varphi \cos 2\varphi + \epsilon_{16} \cos^4\varphi$$
$$+3(\epsilon_{26} - \epsilon_{16}) \cos^2\varphi \sin^2\varphi - \epsilon_{26} \sin^4\varphi. \qquad (B3)$$

The above transformation relations follow from the transformation relations for parameters $A_{\alpha\beta}$ specified in the global and local Cartesian coordinate systems.

Orthorhombic media

Let us consider an orthorhombic medium, whose symmetry planes coincide with the coordinate planes of the global coordinate system. In such a medium, we have

$$\chi_z = \epsilon_{16} = \epsilon_{26} = 0. \qquad (B4)$$

This means that the number of WA parameters specifying P-wave propagation reduces from 9 to 6. If we consider again $\alpha_0^2 = A_{33}$, and thus $\epsilon_z = 0$, the number of WA parameters reduces to 5. The number of the primed WA parameters in the plane (x', z') remains 4, but the transformation relations simplify to:

$$\epsilon'_x = \epsilon_x \cos^4\varphi + \delta_z \cos^2\varphi \sin^2\varphi + \epsilon_y \sin^4\varphi,$$
$$\delta'_y = \delta_y \cos^2\varphi + \delta_x \sin^2\varphi,$$
$$\chi'_z = (\delta_x - \delta_y) \sin\varphi \cos\varphi,$$
$$\epsilon'_{16} = -2\epsilon_x \cos^3\varphi \sin\varphi + 2\epsilon_y \sin^3\varphi \cos\varphi + \delta_z \cos\varphi \sin\varphi \cos 2\varphi. \qquad (B5)$$

Transversely isotropic media with horizontal axis of symmetry (HTI)

In HTI media with axis of symmetry parallel to the x axis, we have, in addition to (B4):

$$\epsilon_y = \epsilon_z = \frac{1}{2}\delta_x, \quad \delta_y = \delta_z. \qquad (B6)$$

The number of WA parameters specifying P-wave propagation reduces from 6 to 3. For $\alpha_0^2 = A_{33}$, and thus $\epsilon_z = 0$, the number of WA parameters reduces to 2. The number of the primed WA parameters in the plane (x', z') remains 4, but the transformation relations further simplify to:

$$\epsilon'_x = \epsilon_x \cos^4\varphi + \delta_y \cos^2\varphi \sin^2\varphi,$$
$$\delta'_y = \delta_y \cos^2\varphi,$$
$$\chi'_z = -\delta_y \sin\varphi \cos\varphi,$$
$$\epsilon'_{16} = -2\epsilon_x \cos^3\varphi \sin\varphi + \delta_y \cos\varphi \sin\varphi \cos 2\varphi. \qquad (B7)$$

Transversely isotropic media with vertical axis of symmetry (VTI)

For completeness, we present here also transformation relations for VTI media. In VTI media, we have, in addition to (B4):

$$\epsilon_x = \epsilon_y = \frac{1}{2}\delta_z, \quad \delta_x = \delta_y. \qquad (B8)$$

The number of WA parameters specifying P-wave propagation is 3 as in the HTI case. For $\alpha_0^2 = A_{33}$, and thus $\epsilon_z = 0$, the number of WA parameters reduces again to 2. The number of the primed WA parameters in the plane (x', z') reduces to two in the VTI case:

$$\epsilon'_x = \epsilon_x, \qquad \delta'_y = \delta_y, \qquad \chi'_z = \epsilon'_{16} = 0. \tag{B9}$$

The primed WA parameters ϵ'_x, δ'_y are equal to the WA parameters ϵ_x, δ_y in the global Cartesian coordinate system.

References

Bakker, P., 2002. Coupled anisotropic shear-wave ray tracing in situations where associated slowness sheets are almost tangent. *Pure appl. Geophys.*, **159**, 1403-1417.

Farra, V., and Pšenčík, I. 2003. Properties of the zero-, first- and higher-order approximations of attributes of elastic waves in weakly anisotropic media. *J. Acoust. Soc. Am.*, **114**, 1366–1378.

Farra, V. and Pšenčík, I., 2008. First-order ray computations of coupled S waves in inhomogeneous weakly anisotropic media. *Geophys. J. Int.*, **173**, 979-989.

Farra, V. and Pšenčík, I., 2010. Coupled S waves in inhomogeneous weakly anisotropic media using first-order ray tracing. *Geophys. J. Int.*, **180**, 405-417.

Farra, V. and Pšenčík, I., 2013. Moveout approximations for P and SV waves in VTI media. *Geophysics*, **78**, WC81–WC92.

Farra, V. and Pšenčík, I., 2013. Moveout approximations for P and SV waves in dip-constrained transversely isotropic media. *Geophysics*, **78**, C53–C59.

Gajewski, D., and I. Pšenčík, 1990. Vertical seismic profile synthetics by dynamic ray tracing in laterally varying layered anisotropic structures. *J. Geophys. Res.*, **95**, 11301–11315.

Grechka, V., Contreras, P. and Tsvankin, I., 2000. Inversion of normal moveout for monoclinic media. *Geophys. Prosp.*, **48**, 577–602.

Klimeš, L., 2006. Common-ray tracing and dynamic ray tracing for S waves in a smooth elastic anisotropic medium. *Stud. Geophys. Geod.*, **50**, 449-461.

Mensch, T. and Rasolofosaon, P., 1997. Elastic-wave velocities in anisotropic media of arbitrary symmetry – generalization of Thomsens parameters ϵ, δ and γ. *Geophys. J. Int.*, **128**, 43–64.

Pšenčík, I., and Gajewski, D., 1998. Polarization, phase velocity and NMO velocity of qP waves in arbitrary weakly anisotropic media. *Geophysics*, **63**, 1754–1766.

Rasolofosaon, P., 2000. Explicit analytic expression for normal moveout from hor-

izontal and dipping reflectors in weakly anisotropic media of arbitrary symmetry type. *Geophysics*, **65**, 1294-1304.

Schoenberg, M. and Helbig, K., 1997. Orthorhombic media: Modeling elastic wave behavior in a vertically fractured earth, *Geophysics*, **62**, 1954–1974.

Schoenberg, M. and Sayers, C. 1995. Seismic anisotropy of fractured rock, *Geophysics*, **60**, 204–211.

Stovas, A., 2010, Generalized moveout approximation for qP- and qSV-waves in a homogeneous transversely isotropic medium: Geophysics, **75**, D79–D84.

Thomsen, L., 1986. Weak elastic anisotropy. *Geophysics*, **51**, 1954–1966.

Tsvankin, I., 1997. Anisotropic parameters and P-wave velocities for orthorhombic media. *Geophysics*, **62**, 1292–1309.

Tsvankin, I., 2001. *Seismic signatures and analysis of reflection data in anisotropic media*. Oxford, Elsevier Science Ltd.

Tsvankin, I. and Thomsen, L., 1994. Nonhyperbolic reflection moveout in anisotropic media. *Geophysics*, **59**, 1290-1304.

Figure captions

Figure 1: HTI model; anisotropy $\sim 26\%$. Variation with the normalized offset $\bar{x} = x/2H$ of relative traveltime errors calculated with the first-order equation (11) ignoring different directions of $\mathbf{N}$ and $\mathbf{n}$ (top), with the first-order equation (13) taking into account different directions of $\mathbf{N}$ and $\mathbf{n}$ (middle) and with the second-order equation (15) (bottom). Relative errors are estimated along profiles with azimuth $\varphi = 0^o$, 30^o, 45^o, 50^o (left), 60^o, 70^o, 80^o and 90^o (right), measured from the x-axis (parallel with the symmetry axis).

Figure 2: HTI model; anisotropy $\sim 26\%$. Top: variation with $\bar{x}$ of exact phase and ray velocities for azimuths $\varphi = 0^o$, 30^o, 45^o, 50^o (left) and 60^o, 70^o, 80^o and 90^o (right), measured from the x-axis (parallel with the symmetry axis). Phase and ray velocity for each φ by the same colour, phase velocity always smaller. Middle: variation of angular differences of exact ray- and phase-velocity directions $\mathbf{N}$ and $\mathbf{n}$ for the same azimuths as above. Bottom: variation of NMO velocity with azimuth φ. Comparison of the first-order formula (17) with (B7) ignoring different directions of $\mathbf{N}$ and $\mathbf{n}$ (blue) and second-order formula (19) with (B7) (red) with exact formula (black).

Figure 3: ORT model; anisotropy $\sim 25\%$. Left column: variation with $\bar{x}$ of relative traveltime errors calculated with the first-order equation (11) ignoring different directions of $\mathbf{N}$ and $\mathbf{n}$ (top), with the first-order equation (13) taking into account different directions of $\mathbf{N}$ and $\mathbf{n}$ (middle) and with the second-order equation (15) (bottom). Relative errors are estimated along profiles with azimuth $\varphi = 0^o$, 30^o, 60^o and 90^o, measured from the x-axis. Right column: Top: variation with $\bar{x} = x/2H$ of exact phase and ray velocities for azimuths $\varphi = 0^o$, 30^o, 60^o and 90^o, measured from the x-axis. Phase and ray velocity for each φ by the same colour, phase velocity always smaller. Middle: variation of angular differences of exact ray- and phase-velocity directions $\mathbf{N}$ and $\mathbf{n}$ for the same azimuths as above. Bottom: variation of NMO velocity with azimuth φ. Comparison of the first-order formula (17) with (B5) ignoring different directions of $\mathbf{N}$ and $\mathbf{n}$ (blue) and second-order formula (19) with (B5) (red) with exact formula (black).

Figure 4: MONO model; anisotropy $\sim 15\%$. Variation with $\bar{x}$ of relative traveltime errors calculated with the first-order equation (11) ignoring different directions of $\mathbf{N}$ and $\mathbf{n}$ (top), with the first-order equation (13) taking into account different directions of $\mathbf{N}$ and $\mathbf{n}$ (middle) and with the second-order equation (15) (bottom). Relative errors are estimated along profiles with azimuth $\varphi = 0^o$, 30^o, 45^o, 60^o, 90^o (left), 90^o, 120^o, 135^o, 150^o and 180^o (right), measured from the x-axis.

Figure 5: MONO model; anisotropy $\sim 15\%$. Top: variation with $\bar{x}$ of exact phase and ray velocities for azimuths $\varphi = 0^o$, 30^o, 45^o, 60^o, 90^o (left) and 90^o, 120^o, 135^o, 150^o and 180^o (right), measured from the x-axis. Phase and ray velocity for each φ by the same colour, phase velocity always smaller. Middle: variation of angular differences of exact ray- and phase-velocity directions $\mathbf{N}$ and $\mathbf{n}$ for the same azimuths as above. Bottom: variation of NMO velocity with azimuth φ. Comparison of the first-order formula (17) with (B3) ignoring different directions of $\mathbf{N}$ and $\mathbf{n}$ (blue) and second-order formula (19) with (B3) (red) with exact formula (black).

Model	α_0(km/s) r^2	β_0(km/s)	ϵ_x δ_x	ϵ_y δ_y	ϵ_{16} δ_z	ϵ_{26} χ_z
HTI	3.805	1.510	-0.169	–	–	–
	0.158		–	-0.373	–	–
ORT	2.437	1.414	0.258	0.328	–	–
	0.337		0.077	-0.083	0.340	–
MONO	2.604	1.566	-0.135	-0.124	0.057	-0.043
	0.362		-0.128	-0.057	-0.241	-0.071

Table 1: Parameters of the models used in tests. α_0 and β_0: P- and S-wave reference velocities; $r^2 = \beta_0^2/\alpha_0^2$; ϵ_x, ϵ_y, ϵ_{16}, ϵ_{26}, δ_x, δ_y, δ_z and χ_z: P-wave WA parameters; $\epsilon_z = 0$.

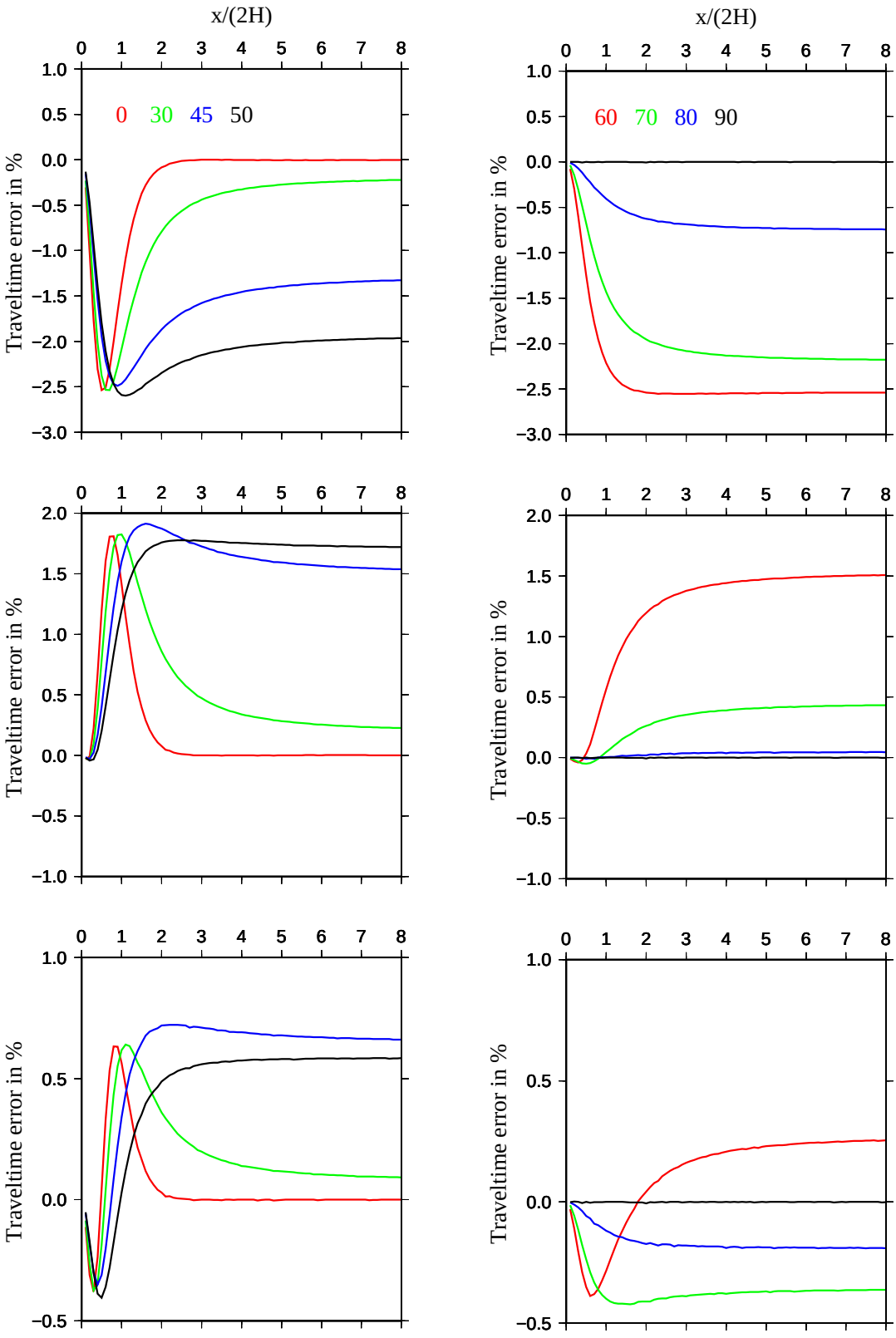

Figure 1: HTI model; anisotropy $\sim$ 26%.

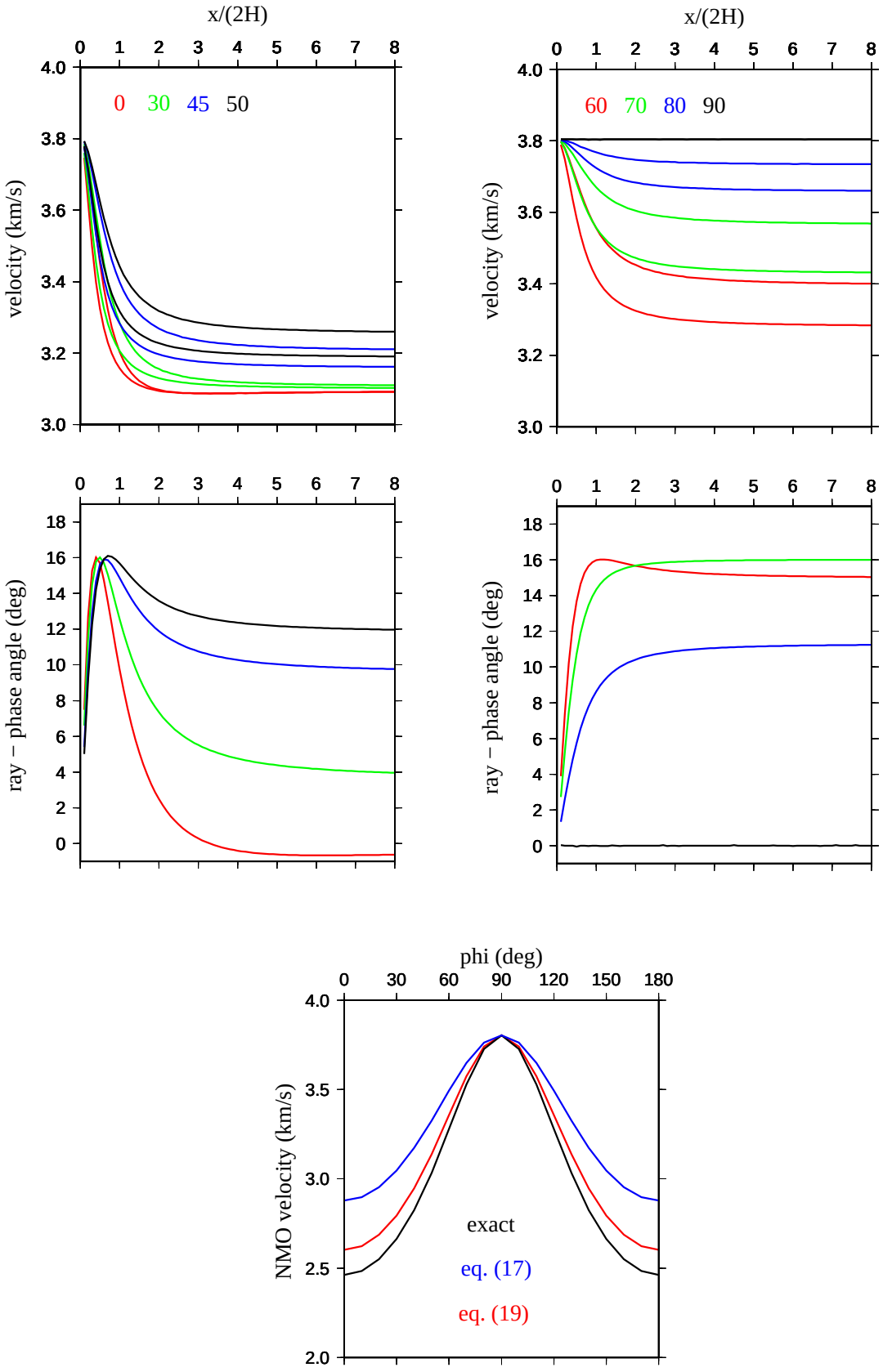

Figure 2: HTI model; anisotropy $\sim 26\%$.

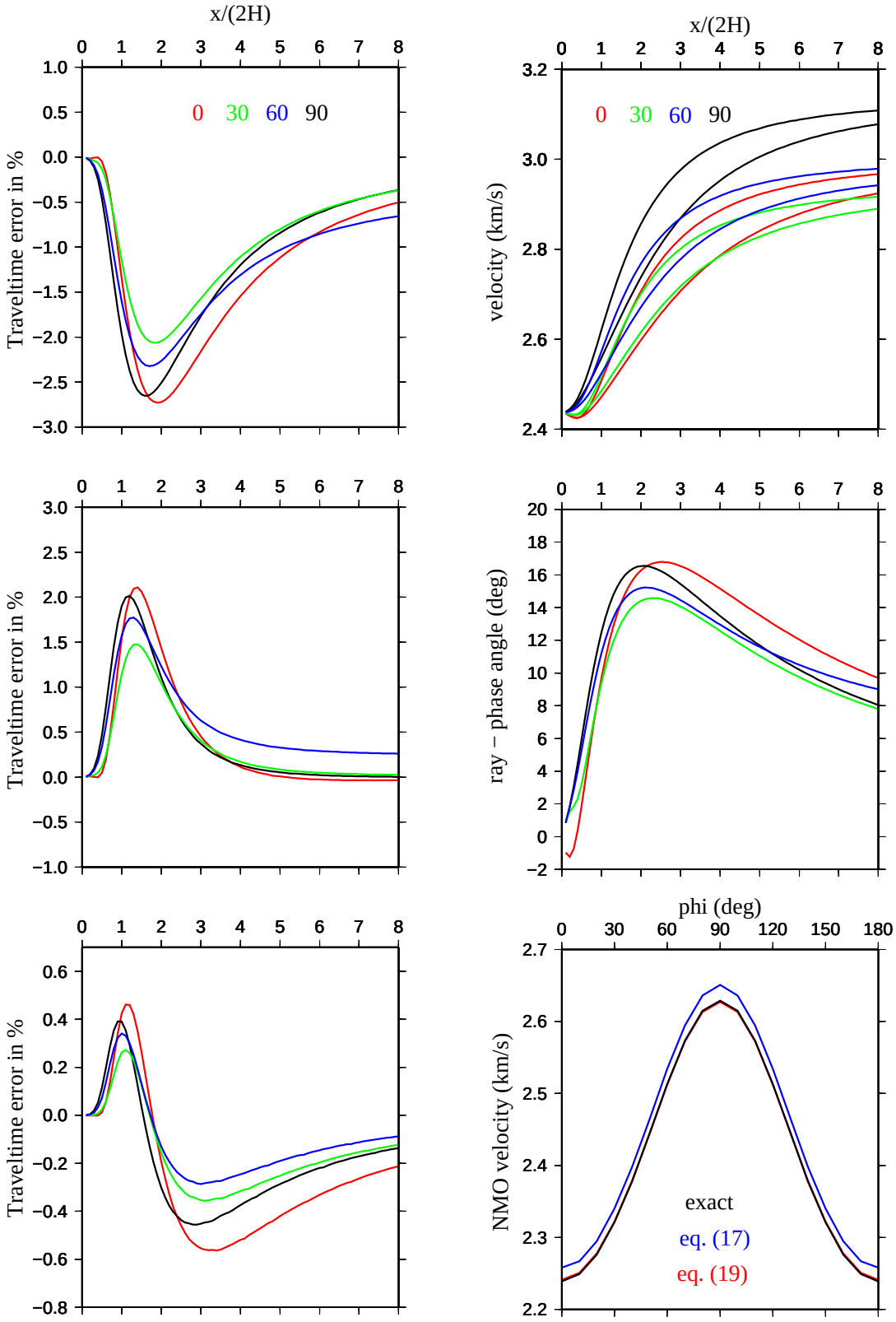

Figure 3: ORT model; anisotropy $\sim 25\%$.

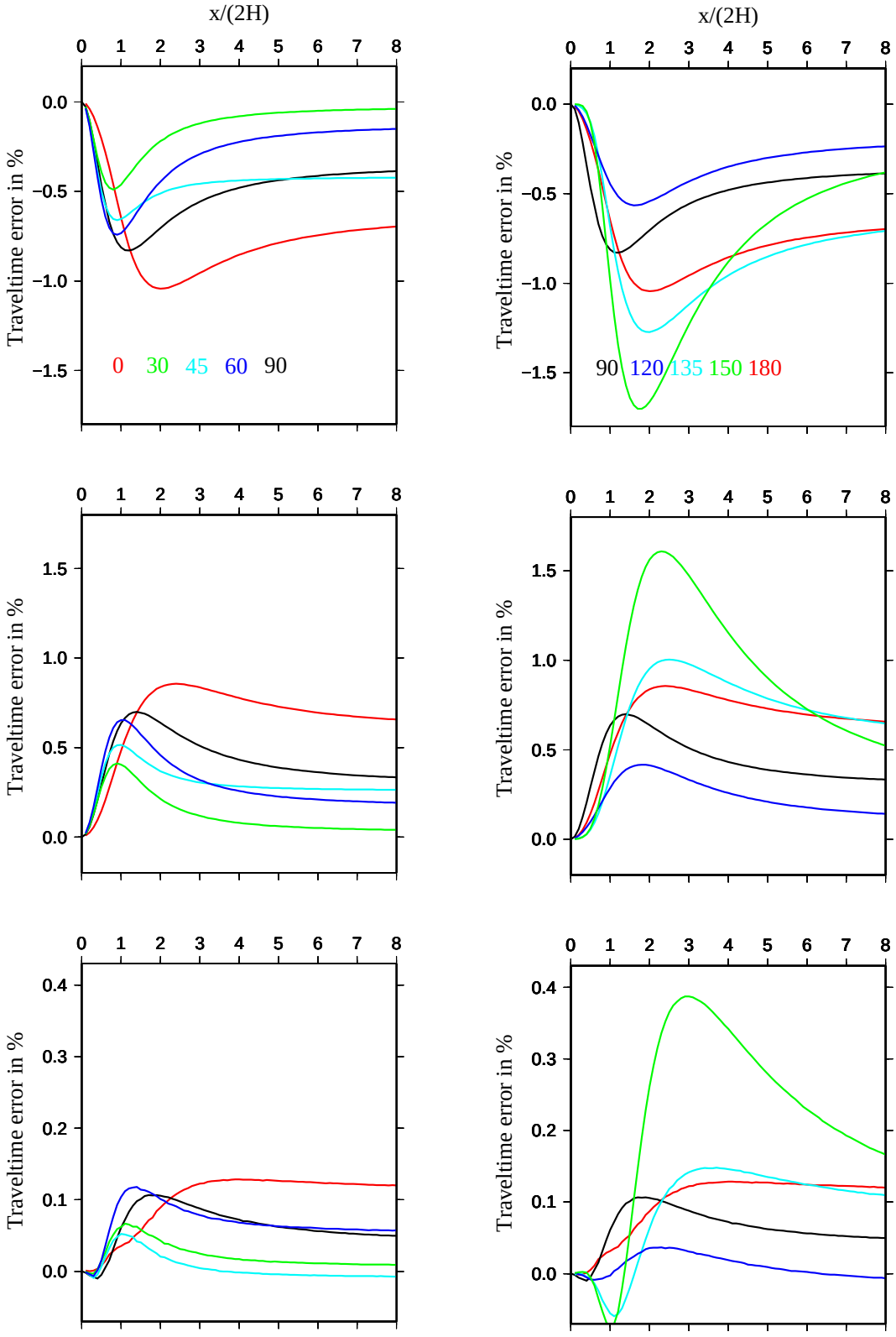

Figure 4: MONO model; anisotropy $\sim$ 15%.

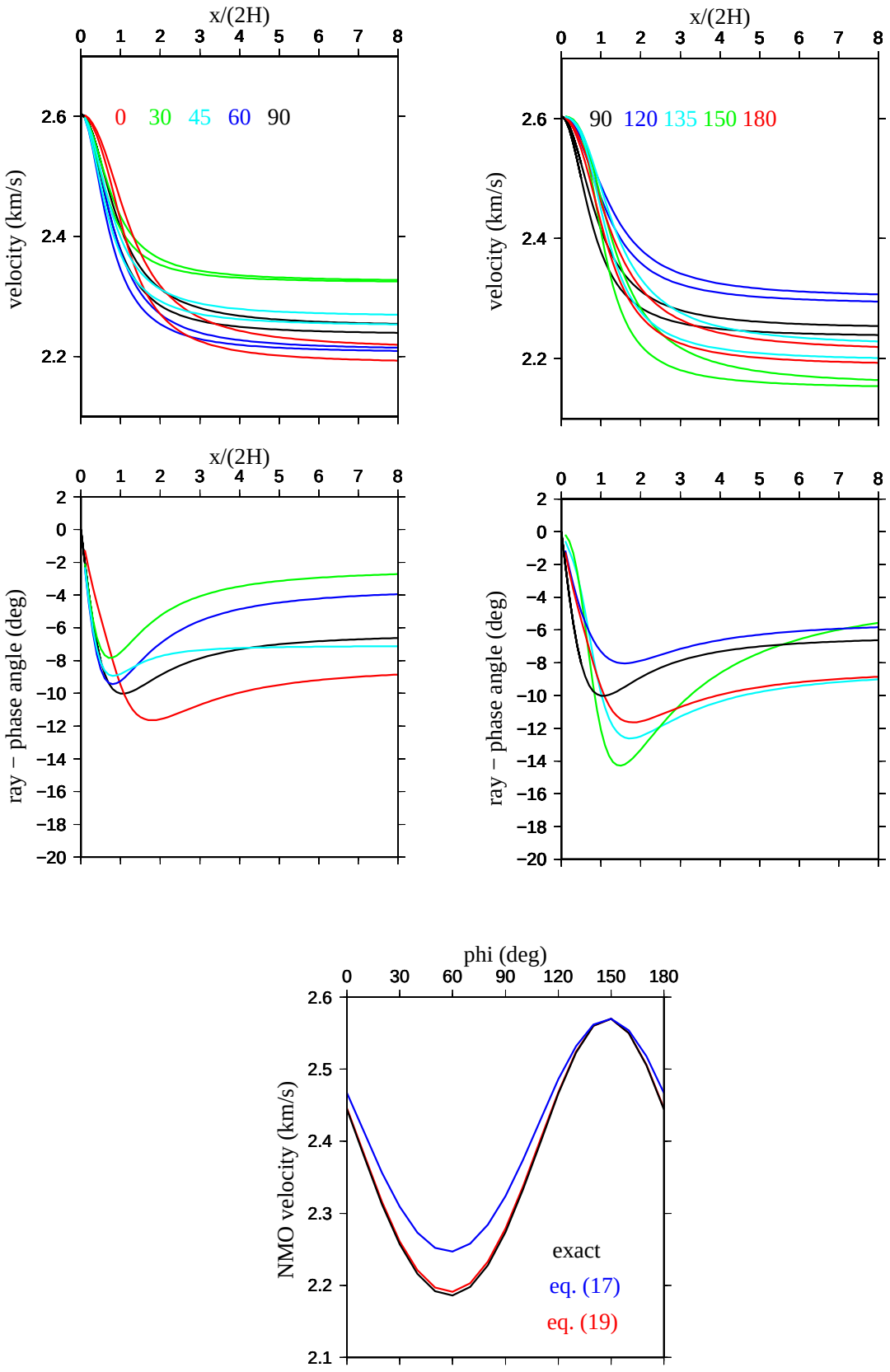

Figure 5: MONO model; anisotropy $\sim 15\%$.